^{222}Rn and ^{226}Ra: indicators of sea-ice effects on air-sea gas exchange

KENT A. FANNING and LINDA M. TORRES

Fanning, K. A. & Torres, L. M. 1991: ^{222}Rn and ^{226}Ra: indicators of sea-ice effects on air-sea gas exchange. Pp. 51–58 in Sakshaug, E., Hopkins, C. C. E. & Øritsland, N. A. (eds.): Proceedings of the Pro Mare Symposium on Polar Marine Ecology, Trondheim, 12–16 May 1990. *Polar Research 10(1)*.

^{222}Rn and ^{226}Ra distributions beneath the sea ice of the Barents Sea revealed that ice cover has varied effects on air-sea gas exchange. Twice, once in late summer and once in late winter, seawater samples from the top meter below drill holes had ^{222}Rn activities that were not lower than their ^{226}Ra activities, indicating the existence of secular equilibrium and a negligible net exchange of ^{222}Rn and other gases with the atmosphere. However, seawater in the upper 20–85 m usually exhibited at least some ^{222}Rn depletion; ^{222}Rn-to-^{226}Ra activity ratios tended to have 'ice-free' values (0.3–0.9) in the summer and values between 0.9 and 1.0 in the winter. Integrated ^{222}Rn depletions and piston velocities in both seasons typically fell in the lower 25% of the ranges for ice-free seawater, suggesting that a moderate but far from total reduction in gas exchange is normally caused by ice cover and/or meltwater. The results demonstrate that sea-ice interference with the oceanic uptake of atmospheric gases such as CO_2 is not well understood and needs further investigation.

Kent A. Fanning and Linda M. Torres, Department of Marine Science, University of South Florida, St. Petersburg, Florida 33701, USA

Introduction

The global significance of the effects of sea-ice cover on air-gas exchange is unresolved at present. A complete absence of atmospheric-CO_2 penetration through sea ice of the Weddell Sea was invoked to help explain why sinking Antarctic Bottom Water appears to carry away only 15% of the anthropogenic excess CO_2 that enters the surface ocean (Poisson & Chen 1987). A partial rather than a complete reduction of gas exchange across sea ice was implied by water-mass studies that found freons F-11 and F-12 to be 20–37% undersaturated in the surface Arctic Ocean (Krysell & Wallace 1988; Wallace et al. 1987). These studies emphasized the consequences of high-latitude gas exchange on oceanic solutes but they did not determine gas-exchange parameters for the air-seawater (or air-ice-seawater) interface.

^{222}Rn is a quantitative tracer of air-sea gas exchange on time scales of a few days (Broecker & Peng 1971, 1974, 1982; Peng et al. 1979; Smethie et al. 1985; Glover & Reeburgh 1987). In a parcel of seawater isolated from exchange with the atmosphere or underlying sediments, activities of ^{222}Rn (A_{222}) and its parent ^{226}Ra (A_{226}) will become equal and attain a condition called *secular equilibrium*. Near the sea surface in the ocean's mixed layer, secular equilibrium is disrupted by the preferential escape of radon to the atmosphere, and the ratio of A_{222} to A_{226} is thus <1.0. A_{222}:A_{226} ratios in ice-free oceanic mixed layers are typically 0.5–0.9, averaging 0.76 ($\pm$0.09) in GEOSECS studies (Peng et al. 1979) and 0.75 ($\pm$0.07) in Transient Tracers' studies (Smethie et al. 1985). The lowest observed ratios are ~0.3 in the Bering Sea (Glover & Reeburgh 1987). *Piston velocity*, which is defined as the thickness of a sea water column exchanging gas with the atmosphere per unit time (Broecker & Peng 1982), ranges over nearly two orders of magnitude in ice-free seawater (Table 1).

The work reported here was a reconnaisance of ^{222}Rn and ^{226}Ra distributions near sea ice. Our objectives were to obtain new insights into the mechanisms of air-sea gas exchange in ice-bearing waters and to estimate the ^{222}Rn depletions and piston velocities in the presence of sea ice for comparison to values for the same exchange parameters in the absence of sea ice.

Materials and methods

The work was done in April 1986 (late winter), and September 1988 (late summer), aboard the Norwegian Coast Guard icebreaker K/V ANDENES during the Norwegian Pro Mare program on the

Table 1. Comparison of ^{222}Rn gas exchange parameters in the Barents Sea in late winter (April) and late summer (September) with ^{222}Rn gas exchange parameters elsewhere in the ocean.

	Barents Sea				Elsewhere		
	Late winter hydrostations		Late summer ice stations		Whole ocean (Ref. 1)	Tropical Atlantic (Ref. 2)	Bering Sea (Ref. 3)
	43	52	2	3			
Depth of ^{222}Rn depletion (m)	110	63	10–20	15–20	48 (±26)	–	–
Total ^{222}Rn depletion (dpm m^{-2})							
Value(s)	280	610	340–680	340–450	190–3610	330–2190	–
Average	–	–	–	–	960	1239	–
Piston velocity (m d^{-1})							
Value(s)	0.6	1.5	1.3–2.6	0.9–1.2	0.5–12.7	1.4–6.9	0.2–4.9
Average	–	–	–	–	2.8	3.6	2.2
Piston velocity (20°C)							
Value(s)	1.2	2.8	2.5–5.1	1.9–2.4	0.6–18.6	1.1–6.0	–
Average	–	–	–	–	3.3	3.1	–

References: (1) Peng et al. (1979). (2) Smethie et al. (1985). (3) Glover & Reeburgh (1987).

Barents Sea. This scheduling permitted a range of sea-ice effects to be examined because of the large seasonal variations in Barents Sea ice cover.

The winter cruise (Fig. 1) investigated the entire water column beneath or adjacent to close-packed winter ice (>90% surface coverage). Seawater in natural or ship-created open areas was sampled with 30-liter Niskin bottles to within 10 m of the bottom. Hydrographic parameters were determined with a CTD or discrete sampling. At an ice station (H1), a helicopter served as transport for collecting seawater below unbroken ice more than 50 miles from the vessel. A small (~10 cm) hole was drilled into the ice, and vacua in gas-tight, 20-liter PVC sampling bottles were used to suck seawater from beneath the ice through weighted tubing (I.D.: 6–12 mm) (Fig. 2).

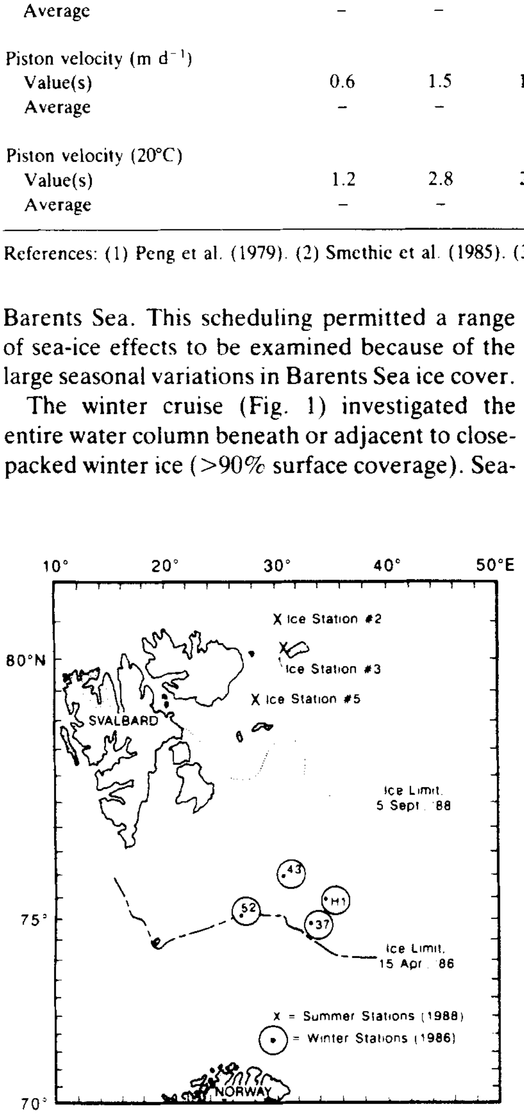

Fig. 1. Map of the Barents Sea showing the station locations during the late winter cruise of April 1986, and the late summer cruise of September 1988. Approximate ice limits are also shown.

The late summer cruise (Fig. 1) consisted entirely of ice stations at which the 1986 ice-station protocol was followed (Fig. 2). Surface ice coverage within the pack was ≤70%.

^{222}Rn activities were determined aboard the vessel after using the 20-liter PVC bottles as ^{222}Rn-extraction chambers (Mathieu et al. 1988) (Fig. 2). Overall ^{222}Rn extraction and counting efficiency was 85%. After the extractions, the seawater samples were slowly passed through columns of Mn-oxide-coated acrylic fiber to extract ^{226}Ra (Reid et al. 1979). Later, the columns were sealed in gas-washing bottles so that the ^{226}Ra activities of the original samples could be determined from the ^{222}Rn ingrown after >1month of storage in accordance with the tests and recommendations of Moore (1981). Relative standard deviations of replicate ^{226}Ra analyses averaged 6%.

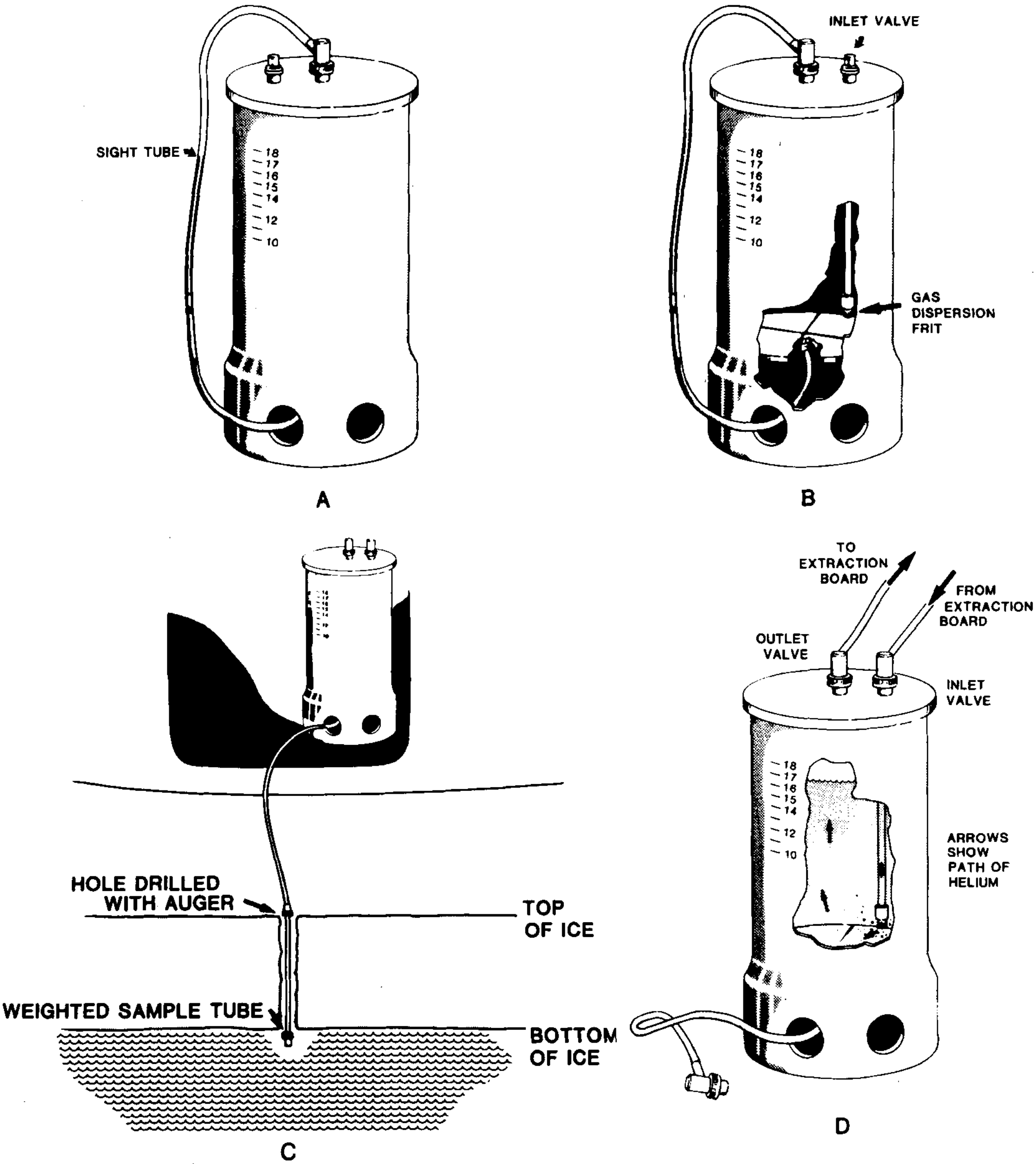

Fig. 2. Diagram of the deployment and use of 20-liter PVC radon sampling and extraction bottles showing: A) an overall view, B) a cutaway view, C) a bottle in sampling position for sucking seawater through weighted tubing lowered into drill holes at ice stations, and D) a radon extraction. Vacua in the bottles were also used to suck seawater from 30-liter Niskin bottles at Pro Mare hydrostations.

Results

The late winter cruise of 1986

Upper portions of the winter ^{222}Rn and ^{226}Ra profiles (Fig. 3) approached secular equilibrium much more closely than reported for ice-free surface water. Out of sixteen samplings of the upper 85 m, ten had $A_{222}:A_{226}$ values higher than the normal range (0.5–0.9), and six had ratios within it. Five of those (two each at hydrostations 43 and 52 and one at ice station H1) exceeded 0.8. These results suggest that the extensive ice cover retarded the degree of degassing. One sample in

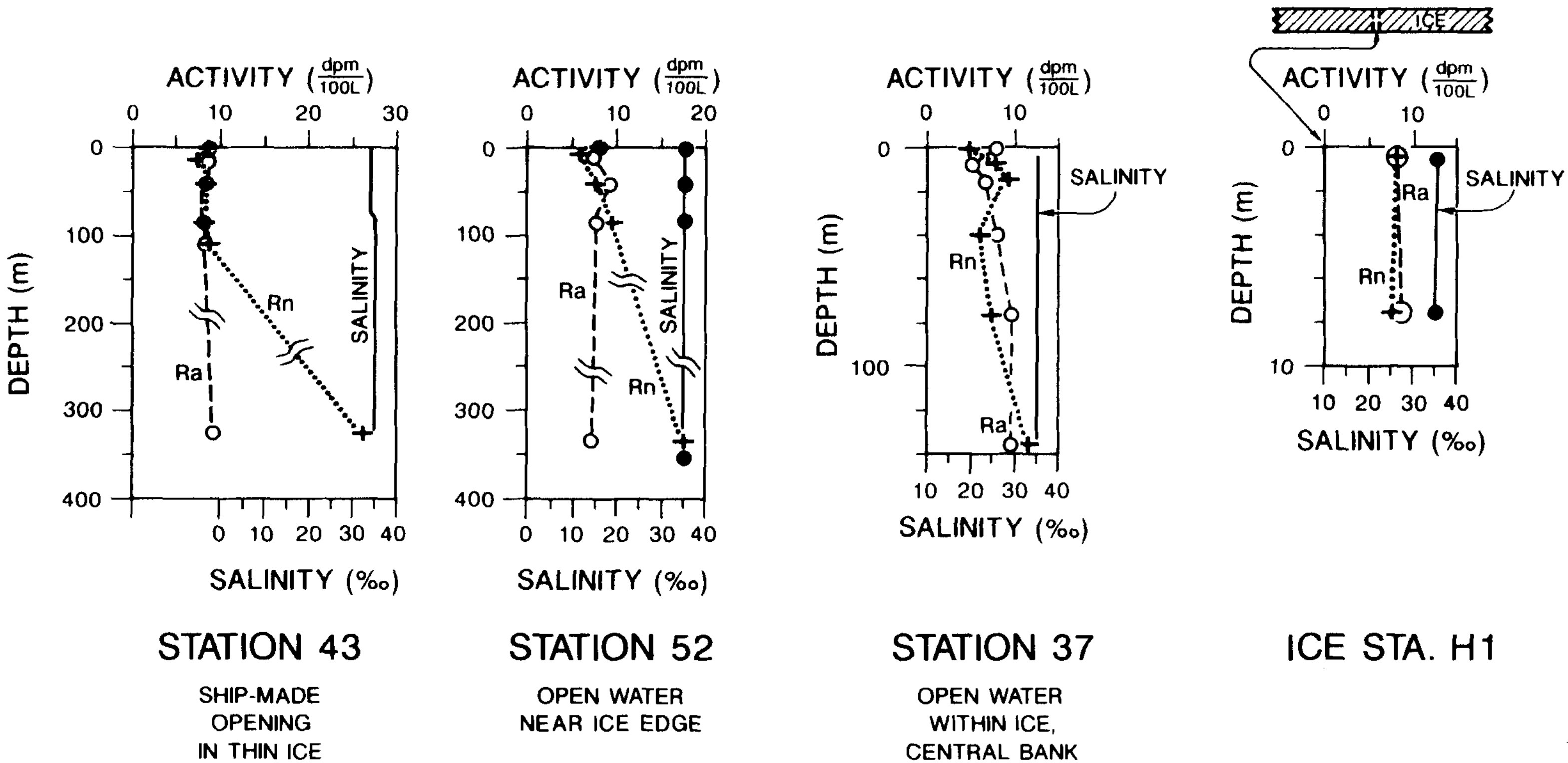

Fig. 3. Profiles of ^{222}Rn activity and ^{226}Ra activity and salinity for the Barents Sea cruise in late winter, April 1986 (hydrostations 43, 52 and 37 and ice station H1). Depths were measured with reference to the sea surface at hydrostations or to the ice surface at ice stations. Seawater rose to within 5 cm of the ice surface in all drill holes. CTD salinity profiles are shown as solid lines without data points; discrete salinity measurements are indicated by solid circles (●).

the upper 20 meters (the 1-m sample at ice station H1) showed clear evidence for secular equilibrium, i.e. no reduction in A_{222} below A_{226}. Another 1-meter sample (at hydrostation 43) had an A_{222} value 4% below its A_{226} value. This sample was close to secular equilibrium, but could also have experienced a small amount of recent exchange. To our knowledge, the water column at hydrostation 43 comes the closest to exhibiting no ^{222}Rn loss to the atmosphere of all oceanic water columns studied to date. Its lowest $A_{222}{:}A_{226}$ value was 0.93 at 10 m; all others in the upper 100 m fell between that value and 1.0.

The strongest winter ^{222}Rn depletions were at hydrostation 37 which had also apparently undergone a recent water-column turnover. A layer in the upper 20 m with a 40–70% ^{222}Rn surplus was both overlain and underlain by seawater with ~20% ^{222}Rn depletion. Large near-bottom ^{222}Rn enrichments at hydrostations 43 and 52 and the small near-bottom enrichment at hydrostation 37 indicated that Barents Sea sediments, as Bering Sea sediments (Glover & Reeburgh 1987) and other shelf sediments (Fanning et al. 1982), emit ^{222}Rn and label near-bottom water with an A_{222} value greater than its A_{226} value. Thus the ^{222}Rn surplus in the seawater at 7–15 m denotes its recent near-bottom origin, and the ^{222}Rn depletion between 40 and 78 m denotes the recent arrival of air-exposed surface water. The water column had little density structure to provide stability, being isohaline (34.5‰ salinity) and almost isothermal (−1.7 to −1.8°C). In addition the water was much shallower than at the other hydrostations (135 m vs. 300–400 m), and the sea surface was ice-free. These three conditions probably led to the overturn and the increased outgassing relative to the other hydrostations.

Depths of the ^{222}Rn-deficient zones beneath the late-winter ice were taken as the depths at which secular equilibrium appeared or were estimated by linear interpolation between the greatest depth showing a ^{222}Rn depletion and the next

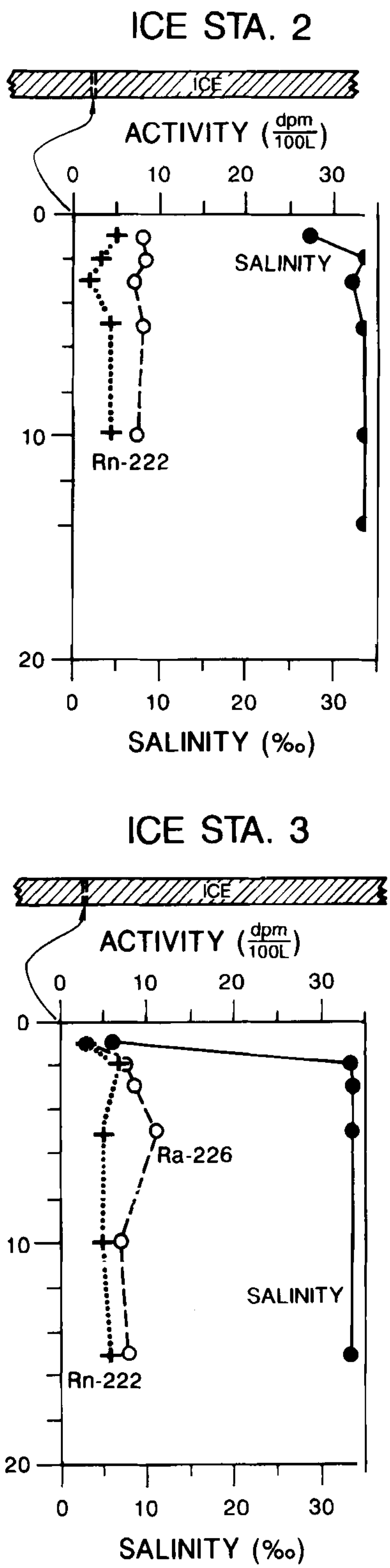

Fig. 4. Profiles of ^{222}Rn activity and ^{226}Ra activity and salinity for the Barents Sea cruise in late summer, September 1988 (ice stations 2 and 3). Depths were measured with reference to the sea surface at hydrostations or to the ice surface at ice stations. Seawater rose to within 5 cm of the ice surface in all drill holes. Discrete salinity measurements are indicated by solid circles (●).

depth sampled (Table 1). The zones extended deeper (60–110 m) than usually observed (Peng et al. 1979) and reached the depletion depths found after storms (Fanning et al. 1982). Salinities at hydrostations 43 and 52 had slight increases from ~34.9‰ above 50 m to ~35.1‰ below 100 m. However the density increases that might have resulted were partially offset by temperature increases from −1 to −2°C above 50 m to ~1.0°C below 100 m, resulting in a weak water-column stability that allowed deeper penetration of gas-exchange processes. The largest pycnocline that was found occurred between 100 and 120 m at hydrostation 43 where σ_t increased by only 0.12. By contrast, σ_t changes over 20-meter-thick pycnoclines in the Bering Sea were ~8 times larger (fig. 3d in Glover & Reeburgh 1987).

The late summer cruise of 1988

Profiles for this cruise indicated much greater individual ^{222}Rn depletions (Fig. 4). Most of the ^{222}Rn-^{226}Ra data pairs from ice stations 2 and 3 had activity ratios in the normal range: 0.5–0.9. Two had very low ratios of 0.30 and 0.37 (the 2-m and 3-m values, respectively, from ice station 2). Not shown is a 1-meter sample taken at ice station 5 (see Fig. 1) with A_{222} = 2.8 dpm (1000 L)$^{-1}$, A_{226} = 7.4 dpm (100 L)$^{-1}$, and $A_{222}:A_{226}$ = 0.38. These low values confirm previous Bering Sea findings that water parcels at high-latitude can undergo considerable ^{222}Rn loss during the summer (Glover & Reeburgh 1987).

The summertime ^{222}Rn losses occurred in ice-melt-stabilized seawater. North of 79° N in the region containing the three ice stations (Fig. 1), Pro Mare CTD casts detected a surface layer in which temperatures were usually less than −1.4°C, and salinities ranged from 33.0‰ to less than 10‰ (Fig. 4). The layer was 20 m thick at most locations. Clearly identifiable thermoclines and haloclines and strong pycnoclines lay between the layer and deeper waters having temperatures between −1 and 0°C and salinities >34‰. The greater openness of the summer ice pack (≤70% coverage) and steady winds from the northwest quadrant at 3–10 m s^{-1} apparently enhanced the degassing in the open areas and the downward and horizontal mixing of the ^{222}Rn-deficient waters in the meltwater layer.

One example of under-ice secular equilibrium was found during the summer cruise. As at the wintertime ice station H1 in Fig. 3, 1-meter water beneath ice station 3 (Fig. 4), showed no reduction of A_{222} below A_{226}. Since the water was obviously meltwater (salinity = 6.1‰), a reasonable explanation is that it was confined to the upper portion of an ice-walled cavity. Otherwise, the mixing processes that were producing and distributing strongly ^{222}Rn-deficient waters throughout the region should have destroyed the strong halocline between 1 and 2 m along with the associated secular equilibrium. Apparently, the combination of solid ice walls and meltwater was capable of restricting ^{222}Rn loss enough to maintain secular equilibrium despite the substantial air-sea ^{222}Rn exchange indicated by the normal-to-extensive ^{222}Rn depletions in the top meter beneath ice stations 2 and 5.

Discussion

^{222}Rn depletions and piston velocities for both summer and winter were calculated by integrating depth profiles (Smethie et al. 1985) for all stations in Figs. 3 and 4 except hydrostation 37 which, due to turnover, was obviously not at steady state. Comparisons were then made to parameters either published in or calculated from previous studies (Table 1). For hydrostations 43 and 52, integrations were made between the surface and the estimated depths of depletion (see above). Time and equipment constraints prevented a more detailed sampling of the water column, resulting in fairly large uncertainties in the measured thicknesses of the ^{222}Rn depletion zones at hydrostations 43 and 52. The consequent errors in the depletions and piston velocities for those stations in Table 1 are estimated to be up to 18% for hydrostations 43 and 30% for hydrostation 52. These values fall in the ranges reported by Smethie et al. (1985).

Because the difficulty of sampling through drill holes precluded the precise determination of depletion depths during the summer cruise, the maximum summertime depletion depth was assumed to be the maximum thickness of the meltwater layer (20 m). This assumption was employed because pycnoclines at the base of the meltwater were 20–40 times the largest 1986 winter pycnocline and 2–5 times the Bering Sea pycnoclines found by Glover & Reeburgh (1987). Thus, parameters for ice stations 2 and 3 in Table 1 are shown with ranges. Low values are based on the average depletions down to the greatest depth sampled, and high values on the assumption that those depletions persisted to 20 meters.

Barents-Sea ^{222}Rn depletions and piston velocities fit within the ranges of those parameters found elsewhere in ice-free seawater. The overall range of Barents Sea ^{222}Rn depletions (280–680 dpm m^{-1}) falls in the lower 14% of the whole-ocean range and the lower 19% of the tropical-Atlantic range. The overall range of Barents Sea piston velocities normalized to 20°C (1.2–5.1 m d^{-1}) falls in the lower 25% of the whole-ocean range, but the highest normalized Barents Sea piston velocity is only 15% below the highest tropical-Atlantic value. Although these comparisons clearly indicate that sea ice restricts gas exchange, Barents Sea parameters are far from the zeros to be expected if sea-ice cover routinely permitted no gas exchange, as required by the Antarctic excess-CO_2 model of Poisson & Chen (1987). Our ^{222}Rn and ^{226}Ra results are much more consistent with the weaker restrictions on gas-exchange implied by the moderate freon undersaturations in the Arctic Ocean (Krysell & Wallace 1988; Wallace et al. 1987). Even at ice-covered hydrostation 43, the upper third of the water column had $A_{222}:A_{226}$ ratios that were uniformly, albeit just slightly, less than unity.

Interestingly, integrated Barents Sea ^{222}Rn depletions and piston velocities varied little between summer and winter, suggesting that the overall effect of sea ice on air-sea gas exchange is roughly the same in both seasons (Table 1). In summer, individual percent depletions were high, but ice meltwater was present to constrain the depth of exchange. In winter, low water-column stability permitted the deeper penetration of ^{222}Rn outgassing to 60–110 m, but the greater ice cover appeared to restrict the degrees of depletion. Probably there was a deep convection followed by a horizontal advection of ^{222}Rn-depleted water associated with the leads that occupy at least 1% of a sea-ice region, even in winter (Smith et al. 1990). The distributions of ^{222}Rn depletions and enrichments at hydrostation 37 (Fig. 3) suggest that the process in those leads might begin with the turnover of a low-stability water column.

Conclusion

From measurements using a ^{222}Rn tracer, our conclusion is that strong retardation of air-sea gas exchange by sea ice occurs mainly in isolated regions on the underside of the ice. The ice structures that produce the isolation are unknown. Normally, even in winter, breaks or other weaknesses in the ice cover seem to be present in sufficient abundance that the integrated gas exchange over the surface water column is slightly less than observed in ice-free seawater. The implication for the possible role of seawater as a sink for anthropogenic CO_2 is that sea ice is a 'porous' barrier to the uptake of CO_2 by high-latitude surface waters having a pCO_2 below the atmospheric value. Poisson & Chen's (1987) assumption of no gas exchange across Weddell Sea ice during the formation of Antarctic Bottom Water is thus open to question, although the lack of an appreciable pCO_2 gradient across Weddell Sea ice may mean that an impermeable ice barrier is not required to explain the low amounts of anthropogenic CO_2 in Antarctic Bottom Water. Until direct studies of ^{222}Rn beneath Weddell Sea ice are performed in winter, the uncertainty regarding the influence of Antarctic sea ice on the fate of atmospheric CO_2 will remain.

Acknowledgements. – Pro Mare provided logistical support. Financial support was provided by the University of South Florida Faculty Research and Creative Scholarship Fund, the American-Scandinavian Foundation, the U.S. National Science Foundation (via grant INT 8900496 to Scripps Institution of Oceanography and grant OCE 9013392 to the University of South Florida), and Pro Mare. C. Rooth supplied valuable comments and suggestions.

References

Broecker, W. S. & Peng, Ts.-H. 1971: The vertical distribution of radon in the BOMEX area. *Earth Planet. Sci. Lett. 11*, 99–108.

Broecker, W. S. & Peng, Ts.-H. 1974: Gas exchange rates between air and sea. *Tellus 26*, 21–35.

Broecker, W. S. & Peng, Ts.-H. 1982: *Tracers in the Sea*, Eldigio Press, Palisades, N.Y.

Fanning, K. A., Breland, J. A., II, & Byrne, R. H. 1982: Radium-226 and radon-222 in the coastal waters of west Florida: concentration and atmospheric degassing. *Science 215*, 667–670.

Glover, D. M. & Reeburgh, W. S. 1987: Radon-222 and radium-226 in southeastern Bering Sea shelf waters and sediment. *Cont. Shelf Res. 7*, 433–456.

Krysell, M. & Wallace, D. W. R. 1988: Arctic ocean ventilation studies with a suite of anthropogenic halocarbon tracers. *Science, 242*, 746–749.

Mathieu, G. G., Biscaye, P. E., Lupton, R. A. & Hammond, D. E. 1988: Measurement of radon-222 in natural water systems. *Health Phys. 55*, 989–992.

Moore, W. S. 1981: Radium isotopes in the Chesapeake Bay. *Estuar. Coast. Shelf Sci. 12*, 713–723.

Peng, Ts.-H., Broecker, W. S., Mathieu, G. G. & Li, Y.-H.

1979: Radon evasion rates in the Atlantic and Pacific oceans as determined during the Geosecs program. *J. Geophys. Res. 84*, 2471–2486.

Poisson, A. & Chen, C.-T. 1987: Why is there little anthropogenic CO_2 in the Antarctic Bottom Water? *Deep-Sea Res. 34*, 1255–1275.

Reid, D. F., Key, R. M. & Schink, D. R. 1979: Radium, thorium and actinium extraction from seawater using an improved manganese-oxide coated fiber. *Earth Planet. Sci. Lett. 43*, 223–226.

Smethie, W. M., Jr., Takahashi, T. & Chipman, D. W. 1985: Gas exchange and CO_2 flux in the tropical Atlantic ocean determined from ^{222}Rn and pCO_2 measurements. *J. Geophys. Res. 90*, 7005–7022.

Smith, S. D., Muench, R. D. & Pease, C. H. 1990: Polynas and leads: An overview of physical processes and environment. *J. Geophys. Res. 95*, 9461–9479.

Wallace, D. W. R., Moore, R. M. & Jones, E. P. 1987: Ventilation of the Arctic Ocean cold halocline: rates of diapycnal and isopycnal transport, oxygen utilization and primary production inferred using chlorofluoromethane distributions. *Deep-Sea Res. 34*, 1957–1979.